

Purinergic control of apical ion conductance by luminal ATP in rat colonic epithelium

Jasmin Ballout, Martin Diener*

Institute for Veterinary Physiology and Biochemistry, Justus Liebig University Giessen, Germany

ARTICLE INFO

Keywords:

ATP
Colonic epithelium
Purinergic receptors
Ion conductances
TRP channels

ABSTRACT

ATP, released e.g. after cell damage or during inflammation, can alter ion transport across the intestinal mucosa via stimulation of purinergic receptors in the basolateral as well as in the apical membrane of epithelial cells. When ATP acts from the serosal side, it induces an increase in short-circuit current (I_{sc}) via Cl^- secretion across the colonic epithelium. In contrast, mucosal ATP or its derivative, BzATP, predominantly stimulating ionotropic P2X₄ and P2X₇ receptors, evoke an increase in I_{sc} , which could not be explained by Cl^- secretion. The underlying ion currents after stimulation of apical purinergic receptors in rat distal colon are still unclear and were investigated in the present study.

Ussing chamber experiments revealed that the I_{sc} induced by mucosal ATP was dependent on the presence of mucosal Ca^{2+} and inhibited by the K^+ channel blocker, Ba^{2+} , indicating the involvement of Ca^{2+} -dependent K^+ channels. Blockade of the transepithelial I_{sc} by lanthanides (La^{3+} , Gd^{3+}) suggests that Ca^{2+} enters the epithelium via nonselective cation channels. Experiments with basolaterally depolarized epithelia confirmed the activation of apical lanthanide-sensitive Na^+ - and Ca^{2+} -permeable cation channels by ATP. Putative candidates might be TRP channels, from which several subtypes were detected in colonic tissue in RT-PCR experiments. In addition, the activation of an apical Cl^- conductance was observed when suitable Cl^- concentration gradients were applied. Consequently, mucosal ATP, acting as 'danger signal', stimulates cation and anion channels in the apical membrane to induce a secretory response as part of the local defence mechanism in the intestinal epithelium.

1. Introduction

Extracellular adenosine triphosphate (ATP) is an important signaling molecule. It can either be released from specific purinergic neurons (Burnstock and Wong, 1978) or as 'danger signal' from damaged cells (Stokes and Surprenant, 2009) thereby acting as paracrine mediator on neighbouring cells. Mechanistically, ATP exerts its actions via two classes of membrane spanning receptors: G-protein coupled P2Y receptors or ionotropic P2X receptors, which function as ligand-gated cation channels (Burnstock, 2018). Each of these classes contain a large number of subtypes (P2Y_{1/2/4/6/11-14} and P2X₁₋₇, respectively).

Beside the well characterized activation of epithelial P2Y receptors (Köttgen et al., 2003), we recently observed that ATP and its derivative BzATP (2'-3'-O-(4-benzoylbenzoyl)adenosine-5'-triphosphate) act on epithelial P2X receptors in the colonic epithelium of rats (Ballout et al., 2022). In Ussing chamber experiments with rat distal colon, both mucosal as well as serosal ATP or BzATP increased the short-circuit current (I_{sc}), a measure for electrogenic ion transport across an

epithelium. Sensitivity to P2X antagonists, such as 5-BDBD (5-(3-bromophenyl)-1,3-dihydro-2H-benzofuro [3,2-e]-1,4-diazepin-2-one; P2X₄ antagonist) or AZ10606120 (N-[2-[[2-[(2-hydroxyethyl)amino]ethyl]amino]-5-quinolinyl]-2-tricyclo [3.3.1.1^{3,7}]dec-1-ylacetamide; P2X₇ antagonist), demonstrated the stimulation of P2X₄ and P2X₇ receptors by serosal and of P2X₇ receptors by mucosal BzATP. RT-PCR and immunohistochemical experiments confirmed the expression of both receptors in the colonic epithelium (Ballout et al., 2022). The transepithelial current induced by mucosal BzATP was not inhibited by the neurotoxin, tetrodotoxin (Ballout et al., 2022). This excludes a secondary activation of secretomotor neurons, which are well known to be involved in the induction of epithelial secretion when purinergic agonists are administered to the serosal compartment (Cuthbert and Hickman, 1985). Interestingly, the I_{sc} evoked by mucosal BzATP was independent from the presence of Cl^- , since it was still present when Cl^- was replaced by the impermeant anion, gluconate. This current was also resistant against bumetanide, a blocker of the basolateral $Na^+-K^+-2Cl^-$ cotransporter which is responsible for the basolateral Cl^- uptake during

* Corresponding author. Institut für Veterinär-Physiologie und -Biochemie, Justus-Liebig-Universität Gießen, Frankfurter Str. 100, Gießen, Germany.

E-mail address: Martin.Diener@vetmed.uni-giessen.de (M. Diener).

<https://doi.org/10.1016/j.ejphar.2024.176941>

Received 15 January 2024; Received in revised form 12 August 2024; Accepted 22 August 2024

Available online 23 August 2024

0014-2999/© 2024 The Authors. Published by Elsevier B.V. This is an open access article under the CC BY license (<http://creativecommons.org/licenses/by/4.0/>).

Table 1
Primers used for RT-PCR analysis of transient receptor potential (TRP) ion channels.

Target	Gene number	Forward	Reverse	Reference
TRPC1	NM_053558	5'-ATAACCAGAAGGAG TTTGTCTCCCAGTC-3'	5'-TCTGACCAAATCAT CCCAATAATCCACAG-3'	Oikawa et al. (2013)
TRPC2	XM_002725704.2	5'-CTGGTGGAACCTCC TGGACGTGGTC-3'	5'-GGATGAACATGAA CCGGATCATGTGCTGC-3'	Oikawa et al. (2013)
TRPC3	NM_021771.2	5'-CAAGAAATCGAGGA TGACAG-3'	5'-GTCTTTTCATTAT CTGCTGATA-3'	Oikawa et al. (2013)
TRPC4	NM_001083115.1	5'-CCGTCAAAAAGAGT TTGTTGC-3'	5'-GCACTGTACTTT ACAAATGCGAC-3'	Oikawa et al. (2013)
TRPC5	NM_080898.3	5'-GAACAACGCCTTCT CCACGCTCTTGA-3'	5'-CTGATAACTTCC TGATAATGTTG-3'	Oikawa et al. (2013)
TRPC6	NM_053559.1	5'-ATACTACAACTGG CCAGGATAAAGTG-3'	5'-CATCATCCTCAAT TTCTGGAATG-3'	Oikawa et al. (2013)
TRPC7	NM_001191691.3	5'-ACTTCACCTACGCC AGGGA-3'	5'-TCCTCGATTTCCT GATAGGAG-3'	Oikawa et al. (2013)
TRPP1	NM_001191934.1	5'-GAGCAGCAACCATA CGCAAG-3'	5'-TGTAGATCCAGC CAGTTCCG-3'	McGahon et al. (2016)
TRPV1	NM_031982.1	5'-TTCTTCTCCGAGG GATTCA-3'	5'-GCTGGGTGGCAT GTCTATCT-3'	Yang et al., 2016
TRPV2	NM_017207.3	5'-ACCGTGACCGACTC TTCAGT-3'	5'-GCTGGCCAGTA AGAGGTAA-3'	Yang et al., 2016
TRPV3	NM_001025757.2	5'-ACGGCGGAGAACGT CTCC-3'	5'-TGTCCGCTTATG GGCC-3'	Yang et al., 2016
TRPV4	NM_023970.1	5'-CCAACCTGTTGAG GGAGAG-3'	5'-TGGCTGCTTCTCT ACGACCT-3'	Yang et al., 2016
TRPV5	NM_053787.3	5'-TGGTGGTCCAGAGA ACAAGA-3'	5'-ATGTGTACGGTT GGCATCAC-3'	Yang et al., 2016
TRPV6	NM_053686.2	5'-TTCGTCAGATGGTT CCACAG-3'	5'-AGTGATCCTGGG CTTGAGTG-3'	Yang et al., 2016
TRPM1	NM_001037733.1	5'-ACCGGGTTGACTTT GTGAAG-3'	5'-TCATCTTCCATT CCAGGAG-3'	Li et al. (2010)
TRPM2	AY749166.1	5'-CTGATCAAGAGGAG GGCTTT-3'	5'-CACACTACCTTCC CTGCATC-3'	Yang et al., 2016
TRPM3	XM_219902.5	5'-GAGAGTGACCCGA TGAAG-3'	5'-TTGAAGTGTTC CTTCGTG-3'	Yang et al., 2016
TRPM4	NM_001,136,229	5'-GAGAGGATCATGAC CCGAAA-3'	5'-GAACTTGCCCCAC ATTAGGA-3'	Yang et al., 2016
TRPM5	XM_344979.4	5'-CAGCAACACCTGGA GAGAGA-3'	5'-AGCCAGTGTGTC AGTCATGG-3'	Yang et al., 2016
TRPM6	XM_219747.6	5'-CAAGAGTGGCTTGT CATCA-3'	5'-TGAACAGGCCAA TCAGCAAAG-3'	Li et al. (2010)
TRPM7	AF375874.1	5'-CTAGCCCTCAGCCA CTGGAC-3'	5'-CCCTGAAAGGAA AAACGTCA-3'	Li et al. (2010)
TRPM8	NM_134371	5'-GCCAGTGATGTGG ACAGTA-3'	5'-ATCTCCTCTGCGT TGTCGTT-3'	Yang et al., 2016
GAPDH	BC059110	5'-CTACAGCAACAGGG TGGTGG-3'	5'-CCACCACCCTGT TGCTGTAG-3'	Pouokam et al. (2013)

Gene numbers refer to <http://www.ncbi.nlm.nih.gov>.

Cl⁻ secretion. Hence, mucosal BzATP does not seem to evoke a typical Cl⁻ secretion which dominates the epithelial response induced by stimulation of basolateral purinergic receptors (Ballout et al., 2022). Further experiments revealed that there must be another explanation for the ATP- or BzATP-induced current in the colonic epithelium, probably via ion channels in the apical membrane (Ballout et al., 2022).

An increased release of ATP has been shown in rodent models of colitis (Wynn et al., 2004) and the augmentation of purinergic signaling is thought to contribute – among other extracellular messengers – to the pathophysiology of inflammatory bowel disease (IBD) (Gulbransen et al., 2012). Consequently, it seemed to be of interest to elucidate the still unclear mechanisms underlying the electrogenic ion transport across rat colonic epithelium after stimulation of apical purinergic receptors with the natural agonist, ATP. For this purpose, Ussing chamber experiments with intact mucosa-submucosa preparations and with basolaterally depolarized epithelia were performed which allow to 'dissect' electrophysiological currents across the apical membrane. These experiments were complemented with RT-PCR experiments to evaluate the expression of TRP (transient receptor potential) ion channels in the colonic epithelium, which turned out as potential downstream target during the course of this study.

2. Material and methods

2.1. Animals

Female and male Wistar rats with a body mass of 180–300 g were used as in previous experiments (Ballout et al., 2022). No differences were observed in the response to apical purine receptor stimulation between both sexes. The animals were bred and housed at the central breeding facility of the Justus-Liebig-University Giessen at an ambient temperature of 22.5 °C and air humidity of 50–55 % on a 12 h: 12 h light-dark cycle with free access to water and food. Animals were killed in CO₂ narcosis by cervical dislocation followed by exsanguination. Experiments were approved by the named animal welfare officers of the Justus Liebig University (administrative number 800_M) and performed according to the German and European animal welfare law.

2.2. Solutions

Most of the Ussing chamber experiments were carried out in a Parsons solution containing in mmol/l: 107 NaCl, 4.5 KCl, 25 NaHCO₃, 1.8 Na₂HPO₄, 0.2 NaH₂PO₄, 1.25 CaCl₂, 1 MgSO₄ and 12.2 glucose. This solution was gassed with carbogen (5 % CO₂ and 95 % O₂, v/v). In the

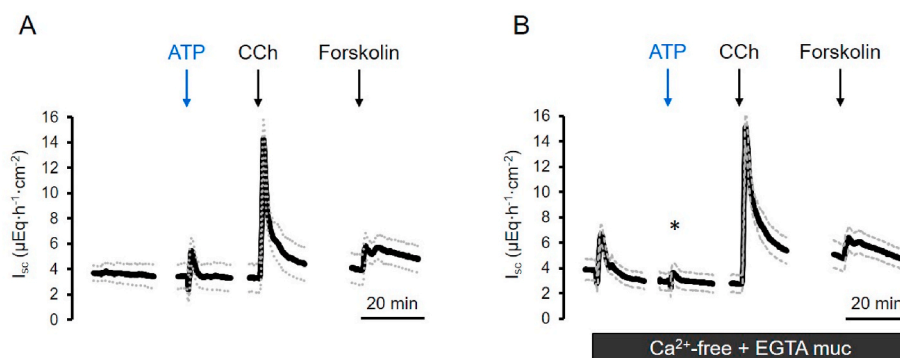


Fig. 1. Effect of ATP (100 $\mu\text{mol/l}$, mucosal) on I_{sc} across mucosa-submucosa preparations of rat distal colon in the presence (A) or absence (B) of mucosal Ca^{2+} (combined with the Ca^{2+} chelator EGTA, 100 $\mu\text{mol/l}$, mucosal). As viability control, carbachol (CCh; 50 $\mu\text{mol/l}$, serosal) and forskolin (10 $\mu\text{mol/l}$, mucosal and serosal) were administered. Data shown in panels A and B are from experiments performed in adjacent tissue samples from the same animals. Line interruptions are caused by omission of time intervals in order to synchronize the tracings of individual records to the administration of the next drug. Data are means (thick lines) \pm S.E.M. (dashed lines), $n = 6$ (all groups); for statistics, see Table 2, * $P < 0.05$ versus response in the presence of mucosal Ca^{2+} .

Ca^{2+} -free Parsons buffer, Ca^{2+} was omitted and 100 $\mu\text{mol/l}$ of the Ca^{2+} chelator EGTA (ethylene glycol bis-(β -aminoethylether) N,N,N',N'-tetraacetic acid) were added. For basolateral depolarization, NaCl was equimolarly replaced by KCl (111.5 mmol/l KCl) in the serosal buffer. For Cl^- free Parsons solution, NaCl and KCl were equimolarly substituted by the corresponding gluconate (Gluc) salts (107 NaGluc/4.5 KGluc or 111.5 mmol/l KGluc, respectively).

In Ussing chamber experiments, where lanthanides were used as putative blockers of cation channels, a HEPES (N-(2-hydroxyethyl) piperazine-N'-2-ethanesulfonic acid)-buffered Tyrode solution was used due to the limited solubility of lanthanides in HCO_3^- - or phosphate-containing buffer (Caldwell et al., 1998). It consisted of (in mmol/l): 140 NaCl, 5.4 KCl, 1.25 CaCl_2 , 1 MgCl_2 , 12.2 glucose, 10 HEPES and was gassed with O_2 . For basolateral depolarization, NaCl was equimolarly substituted by KCl (140 mmol/l KCl). In order to drive Ca^{2+} currents, NaCl in the Tyrode buffer was replaced by 97 mmol/l CaCl_2 . pH of all buffers was set to 7.4 with HCl/NaOH.

2.3. Tissue preparation

The distal colon was dissected and its lumen was flushed several times with ice-cold Parsons solution before it was mounted on a thin plastic rod. A circular incision was made with a blunt scalpel near the distal end. The serosa and the tunica muscularis were stripped off manually in order to obtain mucosa-submucosa preparations. Two segments of the distal colon from each rat were used for Ussing chamber experiments. One segment was treated with putative inhibitors, the other segment was only treated with the respective solvent.

Isolated colonic crypts were prepared as described previously (Ballout et al., 2022). Briefly, a mucosa-submucosa preparation of distal colon was mounted on a holder with tissue adhesive (cyanoacrylate) and incubated for approximately 6 min in Ca^{2+} - and Mg^{2+} -free Tyrode solution containing 10 mmol/l ethylenediaminetetraacetic acid (EDTA) at 37 $^\circ\text{C}$ gassed with ambient air. After incubation, the holder was fixed on a vibrating machine (Chemap, Volketswil, Switzerland) and vibrated once for about 30 s in order to collect isolated crypts under microscopical control before transferring them into lysis buffer for RNA extraction.

2.4. Ussing chamber experiments

Mucosa-submucosa preparations of distal colon were mounted in a modified Ussing chamber filled with 3.5 ml bathing solution on each side, gassed with carbogen (5 % CO_2 and 95 % O_2 , v/v) or O_2 , for Parsons or Tyrode solution, respectively, and incubated at 37 $^\circ\text{C}$. The tissue was short-circuited by a computer-controlled voltage-clamp device (Ingenieur Büro für Mess- und Datentechnik Mussler, Aachen, Germany)

with correction for solution resistance. The exposed tissue surface was 1 cm^2 . Tissue conductance (G_t) was measured every minute by the voltage deviation induced by a current pulse ($\pm 50 \mu\text{A}$, duration 200 ms) under open-circuit conditions as described previously (Bader and Diener, 2018). Short-circuit current (I_{sc}) is expressed as $\mu\text{Eq/h}\cdot\text{cm}^2$, i.e. the flux of a monovalent ion per time and area, with $1 \mu\text{Eq/h}\cdot\text{cm}^2 = 26.9 \mu\text{A}/\text{cm}^2$. An increase in I_{sc} reflects an enhanced secretion of anions or the electrogenic absorption of cations.

Drugs were administered after an equilibration period of about 60 min. The maximal increase in I_{sc} evoked by an agonist is given as the difference to the baseline value just prior administration of the drug (ΔI_{sc}). Baseline values were calculated as mean value over a period of 3 min. At the end of each experiment, the cholinergic agonist, carbachol, and the activator of adenylate cyclases, forskolin, were administered as viability controls.

2.5. RT-PCR

For RT-PCR studies, samples from whole distal colonic wall, isolated colonic crypts from distal colon, duodenal segments, liver, bladder, kidney, or cerebral cortex were transferred into lysis buffer (Macherey-Nagel, Dören, Germany) and homogenized using a mixer mill (NM301; Retsch, Haan, Germany) with a frequency of 30 Hz for about 2 min. Total RNA was extracted using the Nucleo Spin[®] RNA Plus kit (Macherey-Nagel). RNA was transcribed into cDNA with Tetro cDNA synthesis Kit (Bioline, Luckenwalde, Germany).

For the PCR reaction, Bioline[®]Mangomix (Bioline, Germany) was used with 5 mmol/l MgCl_2 . Primers published in the literature (for sequences and references, see Table 1) were obtained from Eurofins MWG Synthesis, Ebersberg, Germany. Each PCR started with a denaturation period at 95 $^\circ\text{C}$ (45 s for the TRPC channels; 30 s for all other tested TRP channels), followed by an annealing phase (TRPC: 55 $^\circ\text{C}$ for 30 s; TRPM: 56 $^\circ\text{C}$ for 45 s; TRPP1: 55 $^\circ\text{C}$ for 45 s; TRPV: 58 $^\circ\text{C}$, 45 s) and an elongation phase at 72 $^\circ\text{C}$ (120 s for the TRPC channels; 90 s for all others); the whole cycle was repeated 35 times. For control of the PCR reaction glyceraldehyde-3-phosphate dehydrogenase (GAPDH) was used; negative controls were performed with RNA/DNA-free water. The reaction product was visualized after electrophoresis in a 3 % (w/v) high resolution agarose gel (Carl Roth, Karlsruhe, Germany) and staining with Roti[®]-Gel Stain (Carl Roth). At least three different biological replicates were performed for each target gene.

2.6. Drugs

Forskolin and ionomycin (Calbiochem, Bad Soden, Germany) were dissolved in ethanol (final maximal ethanol concentration 0.1 % (v/v)).

Table 2
Effects of mucosal ATP on intact colonic epithelia.

	ATP	Carbachol	Forskolin	n
ΔI_{sc} ($\mu\text{Eq}/\text{h}\cdot\text{cm}^2$)				
+ Ca^{2+} - EGTA (muc)	2.02 \pm 0.21	12.32 \pm 1.27	2.02 \pm 0.34	6
- Ca^{2+} + EGTA (muc)	0.96 \pm 0.23 ^a	13.66 \pm 1.19	1.67 \pm 0.51	6
- Ba^{2+}	1.94 \pm 0.35	12.89 \pm 1.21	2.35 \pm 0.53	6
+ Ba^{2+} (ser)	0.26 \pm 0.11 ^a	8.13 \pm 0.19 ^a	0.02 \pm 0.13 ^a	6
- Ba^{2+}	1.94 \pm 0.70	12.00 \pm 4.55	2.10 \pm 0.83	6
+ Ba^{2+} (muc)	0.97 \pm 0.16 ^a	10.21 \pm 1.87	1.96 \pm 0.21	7
-0.1 mM La^{3+}	1.01 \pm 0.33	11.41 \pm 0.60	2.28 \pm 1.40	6
+0.1 mM La^{3+} (muc)	0.71 \pm 0.34	11.47 \pm 1.20	0.65 \pm 0.32	7
-1 mM La^{3+}	0.92 \pm 0.32	12.69 \pm 1.26	0.50 \pm 0.41	6
+1 mM La^{3+} (muc)	0.02 \pm 0.05 ^a	12.66 \pm 2.26	1.38 \pm 0.64	6
- Gd^{3+}	0.85 \pm 0.24	15.39 \pm 1.34	0.23 \pm 0.07	6
+ Gd^{3+} (muc)	0.06 \pm 0.04 ^a	12.61 \pm 1.67	0.18 \pm 0.18	6
- Flufenamate	1.94 \pm 0.79	12.16 \pm 5.91	2.27 \pm 1.70	6
+ Flufenamate (muc)	0.35 \pm 0.17 ^a	12.34 \pm 1.83	3.01 \pm 0.17	6

Increase in I_{sc} (ΔI_{sc}) induced by ATP (100 $\mu\text{mol}/\text{l}$, mucosal), carbachol (50 $\mu\text{mol}/\text{l}$, serosal), and forskolin (10 $\mu\text{mol}/\text{l}$, mucosal and serosal) across mucosa-submucosa preparations of rat distal colon. Responses were tested in the presence of mucosal Ca^{2+} or with a mucosal Ca^{2+} -free buffer containing 100 $\mu\text{mol}/\text{l}$ EGTA, or in the absence or presence of Ba^{2+} (10 mmol/l , mucosal or serosal), La^{3+} (0.1 or 1 mmol/l , mucosal), Gd^{3+} (1 mmol/l , mucosal), or flufenamate (100 $\mu\text{mol}/\text{l}$, mucosal). All experiments were performed in HCO_3^- -buffered Parsons solution, except of the experiments with lanthanides, which were performed in HEPES-buffered Tyrode solution due to the limited solubility of La^{3+} and Gd^{3+} in HCO_3^- or phosphate-containing buffer (Caldwell et al., 1998). Values are given as change in I_{sc} versus baseline (ΔI_{sc}) just prior administration of the individual drug and are means \pm S.E.M. ^a $P < 0.05$ versus response in corresponding control series.

Flufenamic acid was dissolved in 100 mmol/l NaOH. ATP (adenosine 5'-triphosphate disodium salt), carbachol, BaCl_2 , GdCl_3 and LaCl_3 were dissolved in aqueous stock solutions. If not indicated differently, drugs were from Sigma, Taufkirchen, Germany.

2.7. Statistics

Results are given as mean \pm standard error of the mean (S.E.M.) with the number (n) of investigated tissues. For the comparison of two groups either a Student's t-test (unpaired) or a Mann-Whitney-U-test was applied. An F-test decided which test method had to be used. $P < 0.05$ was considered to be statistically significant.

3. Results

3.1. Ca^{2+} -dependence of the secretory response evoked by mucosal ATP

Previous Ussing chamber experiments revealed that ATP or its analogues can activate ionotropic P2X₇ receptors, which are ligand-gated nonselective cation channels, in the apical membrane of the colonic epithelium and thereby induce a transepithelial ion current (Ballout et al., 2022). In order to find out whether a Ca^{2+} influx via these receptors might underlie the resulting ion current, Ca^{2+} in the mucosal buffer was omitted in combination with a Ca^{2+} chelator, EGTA. Under control conditions, ATP (100 $\mu\text{mol}/\text{l}$, mucosal) induced a transient increase in I_{sc} of $2.02 \pm 0.21 \mu\text{Eq}/\text{h}\cdot\text{cm}^2$ (n = 6). This response was significantly diminished by more than 50 % in the absence of mucosal Ca^{2+} (n = 6, $P < 0.05$, Fig. 1). The increase in I_{sc} evoked by the Ca^{2+} -dependent secretagogue carbachol (50 $\mu\text{mol}/\text{l}$, serosal) or the cAMP-dependent secretagogue forskolin (10 $\mu\text{mol}/\text{l}$, mucosal and serosal) were not affected by removal of mucosal Ca^{2+} (Fig. 1, Table 2) excluding an unspecific impairment of the secretory capacity of the epithelium by this manoeuvre.

3.2. Involvement of K^+ channels

A central action site of cytosolic Ca^{2+} are Ca^{2+} -dependent K^+ channels, which upon opening allow a K^+ efflux from the cytosol and thereby induce a membrane hyperpolarization (Keely and Barrett, 2022). Therefore, we tested whether Ba^{2+} , a broad blocker of many types of K^+ channels (Cook and Quast, 1990), interferes with the I_{sc} induced by mucosal ATP (100 $\mu\text{mol}/\text{l}$). Indeed, serosal Ba^{2+} (10 mmol/l) diminished the ATP-induced I_{sc} by more than 85 % ($P < 0.05$, n = 6, Fig. 2, Table 2). Thus, an efflux of K^+ via Ca^{2+} -dependent basolateral K^+ channels might well contribute to the current induced by stimulation of apical purinergic receptors. Surprisingly, Ba^{2+} also inhibited - albeit to a lesser extent - the ATP-induced ion current, when the blocker was administered at the mucosal side. Under these conditions, the ATP response was reduced by 50 % ($P < 0.05$, n = 6, Table 2; see Discussion for possible reasons).

3.3. Effect of blockers of nonselective cation channels

The positive I_{sc} stimulated by mucosal ATP would fit well to the activation of P2X₇ receptors, which have a single channel conductance of about 10 pS in physiological solutions (Riedel et al., 2007). However, an additional possibility could be that the transepithelial I_{sc} induced by mucosal ATP might be amplified by the secondary activation of other nonselective ion conductances, e.g. due to the Ca^{2+} influx or due to

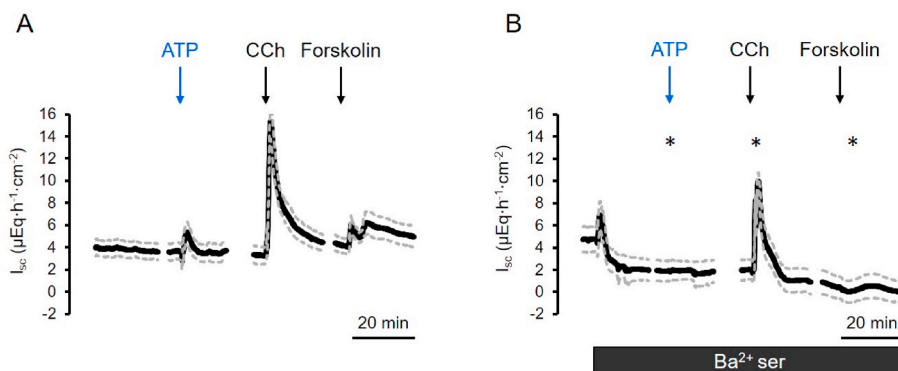


Fig. 2. Effect of ATP (100 $\mu\text{mol}/\text{l}$, mucosal) on I_{sc} across mucosa-submucosa preparations of rat distal colon in the absence (A) or presence (B) of serosal Ba^{2+} (10 mmol/l). As viability control, carbachol (CCh; 50 $\mu\text{mol}/\text{l}$, serosal) and forskolin (10 $\mu\text{mol}/\text{l}$, mucosal and serosal) were administered. Data shown in panels A and B are from experiments performed in adjacent tissue samples from the same animals. Line interruptions are caused by omission of time intervals in order to synchronize the tracings of individual records to the administration of the next drug. Data are means (thick lines) \pm S.E.M. (dashed lines), n = 6 (all groups); for statistics, see Table 2, * $P < 0.05$ versus response in the absence of serosal Ba^{2+} .

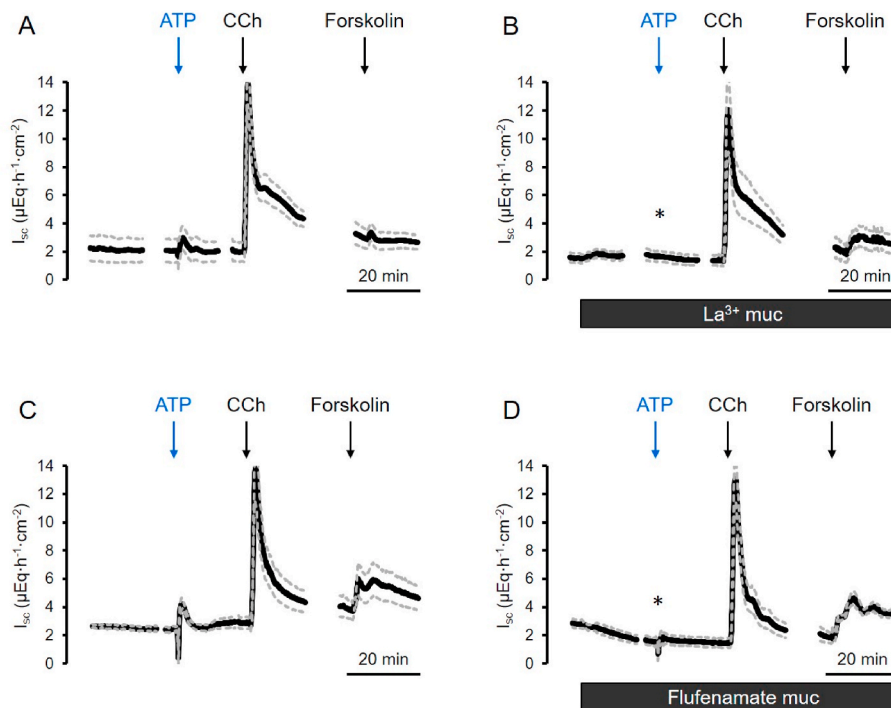


Fig. 3. Effect of ATP (100 $\mu\text{mol/l}$, mucosal) on I_{sc} across mucosa-submucosa preparations of rat distal colon in the absence of any drugs (A, C) or in presence of La^{3+} (B; 1 mmol/l, mucosal) or flufenamate (D; 100 $\mu\text{mol/l}$, mucosal). As viability control, carbachol (CCh; 50 $\mu\text{mol/l}$, serosal) and forskolin (10 $\mu\text{mol/l}$, mucosal and serosal) were administered. Data shown in panels A and B (as well as C and D) are from experiments performed in adjacent tissue samples from the same animals. Line interruptions are caused by omission of time intervals in order to synchronize the tracings of individual records to the administration of the next drug. Data are means (thick lines) \pm S.E.M. (dashed lines), $n = 6$ (all groups); for statistics, see Table 2, * $P < 0.05$ versus response in the absence of any inhibitor.

depolarization. A broad class of nonselective cation channels are the transient receptor potential channels (TRP), from which most are inhibited by lanthanides (IUPHAR Guide to pharmacology). Thus, we screened whether the I_{sc} evoked by mucosal ATP was inhibited by lanthanum (La^{3+}) or gadolinium (Gd^{3+}) ions. Due to the limited solubility of La^{3+} and Gd^{3+} in HCO_3^- - or phosphate-containing buffer (Caldwell et al., 1998), these experimental series were conducted in HEPES-buffered Tyrode solution (for composition, see Methods). Again, in this buffer, ATP (100 $\mu\text{mol/l}$ mucosal) induced an increase in transepithelial I_{sc} which was nearly suppressed in the presence of La^{3+} (1 mmol/l, mucosal; Fig. 3A and B). When used in a 10 times lower concentration (0.1 mmol/l), the lanthanide was ineffective (Table 2). A similar effect, i.e. a nearly complete block of ATP-induced I_{sc} was observed with another lanthanide, Gd^{3+} (Table 2). A chemically different blocker of epithelial nonselective cation channels (Gögelein and Greger, 1986; Gögelein et al., 1990) and of Cl^- conductances (Schultheiss et al., 2000) is flufenamate. Similar to the lanthanides, flufenamate (100 $\mu\text{mol/l}$, mucosal) significantly reduced the I_{sc} stimulated by mucosal ATP by more than 80 % ($P < 0.05$, Fig. 3C and D, Table 2). The currents induced by carbachol or forskolin were not affected by these putative inhibitors of nonselective cation channels (Table 2). Consequently, the ATP-induced ion currents on the apical membrane seem to be (partially) driven by nonselective cation channels.

3.4. Apical ion conductances activated by mucosal ATP

The blocker experiments performed at intact epithelium give only indirect hints about the ionic pathways activated by mucosal ATP as the transepithelial I_{sc} represents the sum of all electrogenic transport processes in a given moment. To study the underlying apical ion conductances in more detail, basolaterally depolarized epithelia were used. Due to its high permeability to potassium, the basolateral membrane is short-circuited under these conditions and the transepithelial current is mainly determined by the conductance of the apical membrane (Fuchs

Table 3

Effect of mucosal ATP on apical Cl^- currents.

HCO ₃ ⁻ -buffered Parsons solution	ATP ΔI_{sc} ($\mu\text{Eq/h}\cdot\text{cm}^2$)	Carbachol	Forskolin	n
KCl ser/NaCl muc	1.00 \pm 0.14	0.06 \pm 0.04	1.29 \pm 0.18	7
KCl ser/NaGluc muc	3.50 \pm 0.63 ^a	0.90 \pm 0.79 ^a	6.34 \pm 1.44 ^a	7
KCl ser/NaGluc muc	2.01 \pm 0.34	0.06 \pm 0.12	2.77 \pm 0.69	7
KGluc ser/NaGluc muc	0.30 \pm 0.10 ^b	0.07 \pm 0.03	0.74 \pm 0.18 ^b	7

Tissues were basolaterally depolarized (serosal: 111.5 mmol/l KCl Parsons or 107 mmol/l KGluc/4.5 mmol/l NaGluc) in the presence (mucosal: 107 mmol/l NaCl/4.5 mmol/l KCl Parsons) or absence (107 mmol/l NaGluc/4.5 mmol/l KGluc Parsons) of mucosal Cl^- . Concentrations were: ATP (100 $\mu\text{mol/l}$, mucosal), carbachol (50 $\mu\text{mol/l}$, serosal), forskolin (10 $\mu\text{mol/l}$, mucosal and serosal). Values are given as increase in I_{sc} versus baseline just prior administration of the individual agonists (ΔI_{sc}). Note that only increases in I_{sc} were calculated (in order to avoid a bias in the analysis of the change evoked by the Cl^- gradient), so that the pronounced negative I_{sc} (K^+ secretion) induced by carbachol (Fig. 5) is not presented. Values are means \pm S.E.M. ^a $P < 0.05$ versus response in the presence of mucosal Cl^- . ^b $P < 0.05$ versus response in the presence of serosal Cl^- .

et al., 1977; Schultheiss and Diener, 1997). When applying appropriate concentration gradients on the epithelium, ion currents can then be driven across different apical membrane conductances.

When tissues were depolarized in the absence of a Cl^- gradient (with 111.5 mmol/l KCl buffer at mucosal and 107 mmol/l NaCl/4.5 mmol/l KCl buffer at serosal side), ATP (100 $\mu\text{mol/l}$ mucosal) induced a positive I_{sc} which amounted to 1.00 \pm 0.14 $\mu\text{Eq/h}\cdot\text{cm}^2$ ($n = 7$, Table 3). This would be consistent with a Na^+ influx into the epithelium through nonselective cation channels in the apical membrane. Subsequent administration of carbachol (50 $\mu\text{mol/l}$ serosal) induced a negative I_{sc} , which is in accordance to the known stimulatory effect of carbachol on apical K^+ channels leading to cellular K^+ efflux (Schultheiss and Diener,

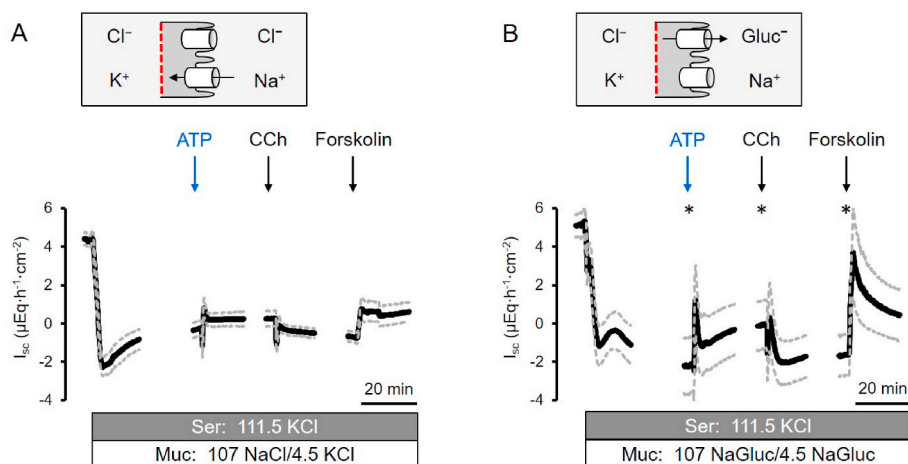


Fig. 4. Effect of ATP (100 $\mu mol/l$, mucosal) on currents across the apical membrane in basolaterally depolarized epithelia. A: Effect on cation currents measured in the absence of any anion concentration gradient (serosal: 111.5 mmol/l KCl Parsons; mucosal: 107 mmol/l NaCl/4.5 mmol/l KCl Parsons). B: Additional effects on apical Cl^- conductance after applying a serosal to mucosal Cl^- gradient (serosal: 111.5 mmol/l KCl Parsons; mucosal: 107 mmol/l NaGluc/4.5 mmol/l KGluc Parsons). As viability control, carbachol (CCh; 50 $\mu mol/l$, serosal) and forskolin (10 $\mu mol/l$, mucosal and serosal) were administered. Data shown in panels A and B are from experiments performed in adjacent tissue samples from the same animals. Line interruptions are caused by omission of time intervals in order to synchronize the tracings of individual records to the administration of the next drug. The insets depict the ionic currents dominating the I_{sc} induced by ATP. Data are means (thick lines) \pm S.E.M. (dashed lines), $n = 7$ (all groups); for statistics, see Table 3, * $P < 0.05$ versus response in the absence of a Cl^- gradient.

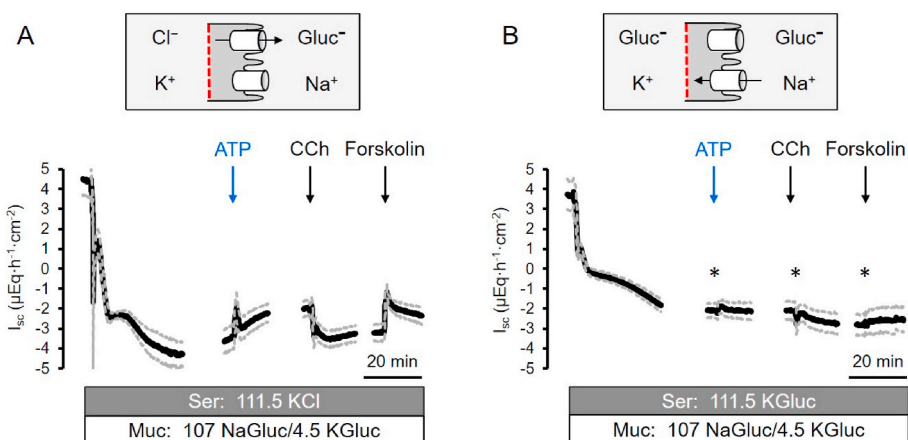


Fig. 5. Effect of ATP (100 $\mu mol/l$, mucosal) on Cl^- currents across the apical membrane in basolaterally depolarized epithelia. Tissues were incubated in the presence (A; serosal: 111.5 mmol/l KCl Parsons; mucosal: 107 mmol/l NaGluc/4.5 KGluc Parsons) or absence (B; serosal: 111.5 mmol/l KGluc Parsons; mucosal: 107 mmol/l NaGluc/4.5 mmol/l KGluc Parsons) of a serosal to mucosal Cl^- concentration gradient. As viability control, carbachol (CCh; 50 $\mu mol/l$, serosal) and forskolin (10 $\mu mol/l$, mucosal and serosal) were administered. Data shown in panels A and B are from experiments performed in adjacent tissue samples from the same animals. Line interruptions are caused by omission of time intervals in order to synchronize the tracings of individual records to the administration of the next drug. The insets depict the ionic currents dominating the I_{sc} induced by ATP. Data are means (thick lines) \pm S.E.M. (dashed lines), $n = 7$ (all groups); for statistics, see Table 3, * $P < 0.05$ versus response in the presence of a Cl^- gradient.

1997). This is followed by a sustained increase in I_{sc} when the activator of adenylate cyclases, forskolin (10 $\mu mol/l$, mucosal and serosal) was administered (Fig. 4A), and is consistent with the activation of nonselective cation channels allowing Na^+ influx into the epithelium (Siemer and Gögelein, 1993). In order to find out, whether mucosal ATP might in addition activate a Cl^- current across the apical membrane, mucosal Cl^- was replaced by gluconate in order to create a strong serosal to mucosal Cl^- gradient. Under these conditions, the effect of mucosal ATP on I_{sc} across the apical membrane was significantly enhanced by more than 2.5fold ($P < 0.05$). The long-lasting negative I_{sc} (K^+ efflux) induced by carbachol was preceded by a positive current consistent with the activation of Ca^{2+} -dependent Cl^- channels (for review see Dulin, 2020). The response to forskolin was significantly enhanced by a factor of 5 (Fig. 4B–Table 3). This is consistent with the well-known activation of apical cystic fibrosis transmembrane conductance regulator (CFTR) Cl^-

channels after cAMP/protein kinase A-dependent phosphorylation (for review see Csanády et al., 2019).

In order to prove that this enhancement of ionic currents across the apical membrane was indeed carried by a Cl^- flux through apical anion channels, Cl^- was removed from the serosal compartment and substituted by the impermeant anion gluconate. In the corresponding control series with a serosal to mucosal Cl^- concentration gradient (111.5 mmol/l KCl serosal; 107 mmol NaGluc/4.5 mmol/l KGluc mucosal), ATP (100 $\mu mol/l$, mucosal) induced a transient increase in I_{sc} , which amounted to $2.01 \pm 0.34 \mu Eq/h \cdot cm^2$ ($n = 7$; Fig. 5A, Table 3). When Cl^- was substituted by gluconate in the serosal compartment (111.5 mmol/l KGluc serosal; 107 NaGluc/4.5 mmol/l KGluc mucosal), the ATP-induced current across the apical membrane was strongly inhibited (Fig. 5B). The same held true for the response to carbachol, where the long-lasting fall in I_{sc} was diminished, as well as the apical

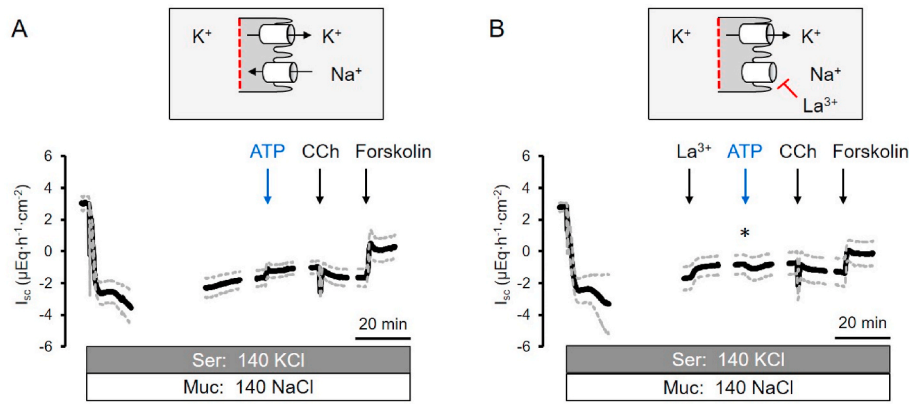


Fig. 6. Effect of ATP (100 µmol/l, mucosal) on cation currents across the apical membrane I_{sc} in basolaterally depolarized epithelia. Tissues were basolaterally depolarized by high K^+ concentration in the serosal compartment (140 mmol/l KCl Tyrode) and with 140 mmol/l NaCl Tyrode in the mucosal compartment in the absence (A) or presence (B) of La^{3+} (1 mmol/l, mucosal). As viability control, carbachol (CCh; 50 µmol/l, serosal) and forskolin (10 µmol/l, mucosal and serosal) were administered. Data shown in panels A and B are from experiments performed in adjacent tissue samples from the same animals. Line interruptions are caused by omission of time intervals in order to synchronize the tracings of individual records to the administration of the next drug. The insets depict the ionic currents dominating the I_{sc} induced by ATP. Data are means (thick lines) \pm S.E.M. (dashed lines), $n = 7$ (control series) or $n = 8$ (series with La^{3+}); for statistics, see Table 4.

Table 4
Effect of mucosal ATP on apical cation currents.

Target	HEPES-buffered Tyrode solution	ATP ΔI_{sc} (µEq/h.cm ²)	Carbachol	Forskolin	n	
$I_{R/Cat}^{pp}$	KCl ser/ NaCl muc	-	0.78 \pm	-1.83 \pm	2.40 \pm 0.80	8
	La^{3+}	0.22	0.18			
	+	-0.41 \pm	-1.51 \pm	1.53 \pm 0.47	7	
$I_{R/Cat}^{pp}$	KCl ser/ NaCl muc	-	0.22 ^a	0.25		
	Gd^{3+}	0.18	0.19			
	+	-0.55 \pm	-1.53 \pm	0.66 \pm 0.20	6	
I_{Ca}^{pp}	KCl ser/97 CaCl ₂ muc	-	0.20 ^a	0.27		
	Gd^{3+}	0.20 ^a	0.27			
	+	0.81 \pm	-1.28 \pm	4.50 \pm 1.48	7	
	La^{3+}	0.18	0.14			
	+	0.03 \pm	-1.14 \pm	1.85 \pm	9	
	La^{3+}	0.03 ^a	0.17	0.45 ^{P = 0.06}		

Tissues were basolaterally depolarized (140 mmol/l KCl Tyrode serosal). Mucosal solutions were: 140 mmol/l NaCl Tyrode (for $I_{R/Cat}^{pp}$) or 97 mmol/l CaCl₂ (for I_{Ca}^{pp}). Concentrations were: ATP (100 µmol/l, mucosal; 50 µmol/l for the measurements of I_{Ca}^{pp}), carbachol (50 µmol/l, serosal), forskolin (10 µmol/l, mucosal and serosal), La^{3+} (1 mmol/l, mucosal), Gd^{3+} (1 mmol/l, mucosal). Values are given as change in I_{sc} versus baseline just prior administration of the individual agonist (ΔI_{sc}) and are means \pm S.E.M. ^a $P < 0.05$ versus response of the same agonist in the corresponding control series.

current stimulated by forskolin, which was nearly abolished (Fig. 5B–Table 3). Consequently, also Na^+ and Cl^- currents across the apical membrane are modulated by mucosal ATP.

3.5. Involvement of nonselective cation channels on apical ion currents induced by ATP

Inhibition of the ATP-induced transepithelial current by lanthanides (Fig. 3A and B, Table 2) suggests the activation of nonselective cation conductance(s) after stimulation of apical purinergic receptors. In order to prove this hypothesis more directly, experiments with basolaterally depolarized epithelia were performed. In the initial series of experiments, tissues were depolarized with a 140 mmol/l KCl Tyrode solution at the serosal side and with a 140 mmol/l NaCl Tyrode solution at the mucosal side allowing either a K^+ efflux ($I_{R/Cat}^{pp}$) via apical K^+ channels leading to a negative I_{sc} or a Na^+ flux into the epithelium via nonselective cation channels (I_{CaT}^{pp}) leading to a positive I_{sc} . Under these conditions and in the absence of La^{3+} , ATP (100 µmol/l mucosal) and forskolin (10 µmol/l mucosal and serosal) induced a positive I_{sc} , which

would be consistent with a stimulation of Na^+ influx across the apical membrane. In contrast, carbachol induced a pronounced negative I_{sc} , which amounted to -1.83 ± 0.18 µEq/h.cm², Fig. 6A) being consistent with a K^+ efflux across Ca^{2+} -dependent K^+ channels (Schultheiss and Diener, 1997). The positive current across the apical membrane induced by ATP was reverted into a negative current, when the epithelia were pretreated with La^{3+} (1 mmol/l, mucosal; Fig. 6B–Table 4). The same was observed with Gd^{3+} (1 mmol/l, mucosal; Table 4). The forskolin-induced current across the apical membrane was only numerically reduced under these conditions, whereas the carbachol-induced current ($I_{R/Cat}^{pp}$) was not affected by the lanthanides (Table 4).

The dependence of the I_{sc} evoked by mucosal ATP on the availability of mucosal Ca^{2+} (Fig. 1, Table 2) suggests that Ca^{2+} influx via the apical membrane plays a central role in the response to the purinergic agonist. In order to prove this hypothesis, apical Ca^{2+} currents were measured in basolaterally depolarized epithelia with Ca^{2+} as the only permeant cation in the mucosal compartment (serosal: 140 mmol/l KCl Tyrode, mucosal: 97 mmol/l CaCl₂ Tyrode). For these series of experiments, the concentration of ATP had to be reduced to 50 µmol/l, as the viability of the tissue was strongly reduced after administration of higher concentrations indicated by a strong increase in tissue conductance. Indeed, mucosal ATP stimulated a (Ca^{2+} -carried) positive I_{sc} , which was suppressed when tissues were pretreated with La^{3+} (1 mmol/l, mucosal; Fig. 7, Table 4). This putative Ca^{2+} current was further enhanced by forskolin (Fig. 7), a response which was – at least numerically – reduced by about 60 % in the presence of La^{3+} (Table 4). Interestingly, this forskolin response was concomitant with a prominent increase in tissue conductance (from 26.7 ± 2.2 mS/cm² to 87.0 ± 15.4 mS/cm², $n = 9$) leading to high transepithelial I_{sc} in some tissues as indicated by the large scatter of the I_{sc} curve depicted in Fig. 7A. This was not observed when Ca^{2+} influx was prevented by La^{3+} (see Discussion). In the presence of the lanthanide, forskolin induced only a moderate increase in G_t (from 26.0 ± 2.5 mS/cm² to 38.1 ± 4.4 mS/cm², $n = 7$), which has to be expected after the presumed activation of apical cation channels. Thus, in the ion current evoked by ATP, nonselective cation channels (permeable for Ca^{2+} and Na^+) might be involved, where the large family of TRP channels are possible candidates for.

3.6. Expression of TRP channels in colonic epithelium

Expression of TRP channels was investigated with RT-PCR experiments. In the case of TRPC channels, only a weak signal for TRPC6 was found in homogenates from intact colon (Fig. 8A), whereas no signal

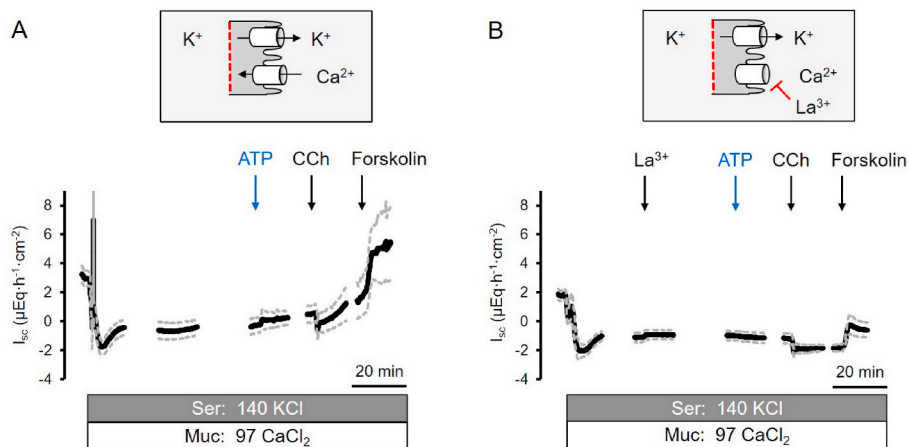


Fig. 7. Effect of ATP (50 $\mu\text{mol/l}$, mucosal) on Ca^{2+} currents across the apical membrane I_{sc} in basolaterally depolarized epithelia. Tissues were incubated in the presence of a Ca^{2+} gradient (serosal: 140 mmol/l KCl Tyrode; mucosal: 97 mmol/l CaCl_2 Tyrode) in the absence (A) or presence (B) of La^{3+} (1 mmol/l, mucosal). As viability control, carbachol (CCh; 50 $\mu\text{mol/l}$, serosal) and forskolin (10 $\mu\text{mol/l}$, mucosal und serosal) were administered. Data shown in panels A and B are from experiments performed in adjacent tissue samples from the same animals. Line interruptions are caused by omission of time intervals in order to synchronize the tracings of individual records to the administration of the next drug. The insets depict the ionic currents dominating the I_{sc} induced by ATP. Data are means (thick lines) \pm S.E.M. (dashed lines), $n = 7$ (series with La^{3+}) or $n = 9$ (control series); for statistics, see Table 4.

could be detected for TRPC5 or TRPC7 (Fig. 8A) as well as for TRPC1 to TRPC4 (data not shown). An amplificate of the expected size for TRPP1 was detected both in colonic homogenates and in isolated colonic crypts (Fig. 8B). In the case of TRPV channels, TRPV3, TRPV4 and TRPV6 were detected both in colonic homogenates and in isolated colonic crypts, whereas TRPV2 was only found in homogenates from intact colon (Fig. 9). For TRPM channels, amplificates for TRPM3, TRPM4, TRPM6, and TRPM7 were present in colonic epithelium (Fig. 10). Weak signals for TRPM2 and TRPM5 of the expected size were observed, too; however, the presence of additional, unspecific bands makes the interpretation questionable. No amplificates for TRPM1 or TRPM8 were found (Fig. 10). Primer free PCR (water) did not reveal any products. Primers for GAPDH were used to proof the quality of the RT-PCR reaction (Figs. 8–10). Cerebral cortex, duodenum, kidney, liver, or urinary bladder were used as reference tissue (Li et al., 2010; Yang et al., 2016; McGahon et al., 2016).

3.7. Activation mechanisms of the La^{3+} -sensitive apical cation conductance

Activation of apical ionotropic purinergic receptors will depolarize the membrane via cation influx and also evoke an increase in the cytosolic Ca^{2+} concentration. In order to find out, which of these mechanisms might be involved in the activation of the La^{3+} -sensitive apical nonselective cation conductance, experiments with a Ca^{2+} ionophore, ionomycin, and apical depolarization were performed. Indeed, ionomycin (1 μM , mucosal) induced a transient increase in I_{sc} , which amounted to $1.52 \pm 0.34 \mu\text{Eq/h}\cdot\text{cm}^2$ ($n = 6$; Fig. 11A). This current was completely suppressed after pretreatment of the tissue with La^{3+} (1 mM, mucosal; $P < 0.05$; Fig. 11B).

Depolarization of the apical membrane by KCl (30 mM, mucosal; Fig. 11C and D) induced a long-lasting increase in I_{sc} which has to be expected when shifting the membrane potential of the apical membrane to more depolarized values. However, this current was resistant to La^{3+} ($1.29 \pm 0.19 \mu\text{Eq/h}\cdot\text{cm}^2$ in the absence and $0.81 \pm 0.18 \mu\text{Eq/h}\cdot\text{cm}^2$ in the presence of the lanthanide, $n = 6$, difference not significant). The success of the apical depolarization was indicated by the loss (Fig. 11D) or even reversal (Fig. 11C) of the forskolin-induced I_{sc} into a negative current (Fig. 11D). This has to be expected when the driving force for Cl^- efflux, i.e. an apical membrane potential more negative than the Cl^- equilibrium potential, is reversed. Consequently, a sole depolarization is not sufficient to activate the La^{3+} -sensitive apical cation conductance.

4. Discussion

The underlying ionic mechanisms after stimulation of apical purinergic receptors in the colonic mucosa were investigated in this study. The effect of ATP was strongly dependent on the presence of mucosal Ca^{2+} , which fits well to the increase in cytosolic Ca^{2+} concentration observed after stimulation of purinergic receptors in isolated colonic crypts (Ballout et al., 2022). The dominant response to an increase of cytosolic Ca^{2+} concentration in these cells is the activation of Ca^{2+} -dependent K^+ channels (Keely and Barrett, 2022) leading to a pronounced membrane hyperpolarization. This promotes the driving force for Cl^- efflux (Böhme et al., 1991) as well as the driving force for Na^+ influx via cation channels (see below), both leading to an enhanced I_{sc} in Ussing chamber experiments. The strong inhibition (by more than 85%; Fig. 2) of the ATP-induced I_{sc} by the K^+ channel blocker, Ba^{2+} , fits well to this mechanism. Also mucosal Ba^{2+} (applied to block apical K^+ channels) reduced the response to mucosal ATP, albeit to a lesser extent (Table 2). However, activation of apical K^+ channels, when occurring alone, would lead to a negative I_{sc} , which is not in accordance with the measured ATP-induced rise in transepithelial current. Thus, this result seems to be paradox at first glance. One reason for this unexpected finding might be that Ba^{2+} is known to inhibit agonist binding to P2X₇ receptors (Virginio et al., 1997) so that the electrogenic response evoked by receptor activation will be reduced. Another alternative explanation might be that also apical K^+ channels can – to a certain extent – enhance anion secretion and thereby increase transepithelial I_{sc} (Cook and Young, 1989), as they form an additional “electrical battery” driving the flux of Cl^- across the apical membrane.

In our previous study, the I_{sc} induced by stimulation of apical P2X₇ receptors in intact epithelium was not significantly reduced by typical manoeuvres inhibiting Cl^- secretion such as Cl^- substitution or bumetanide, the blocker of the basolateral $\text{Na}^+-\text{K}^+-2\text{Cl}^-$ cotransporter responsible for Cl^- accumulation in the colonic epithelium (Ballout et al., 2022). However, the present results demonstrate that a small Cl^- secretory component can be revealed under adequate conditions. In tissues, in which the basolateral membrane had been electrically ‘eliminated’ by K^+ depolarization, mucosal ATP induced an increase in I_{sc} across the apical membrane when an adequate Cl^- driving force was present (Figs. 4B and 5A). This current was abolished after substitution of mucosal Cl^- by the impermeant anion, gluconate (Fig. 5B–Table 3). The responses to carbachol and forskolin, two well-known secretagogues leading to a Cl^- secretion via two distinct signal pathways,

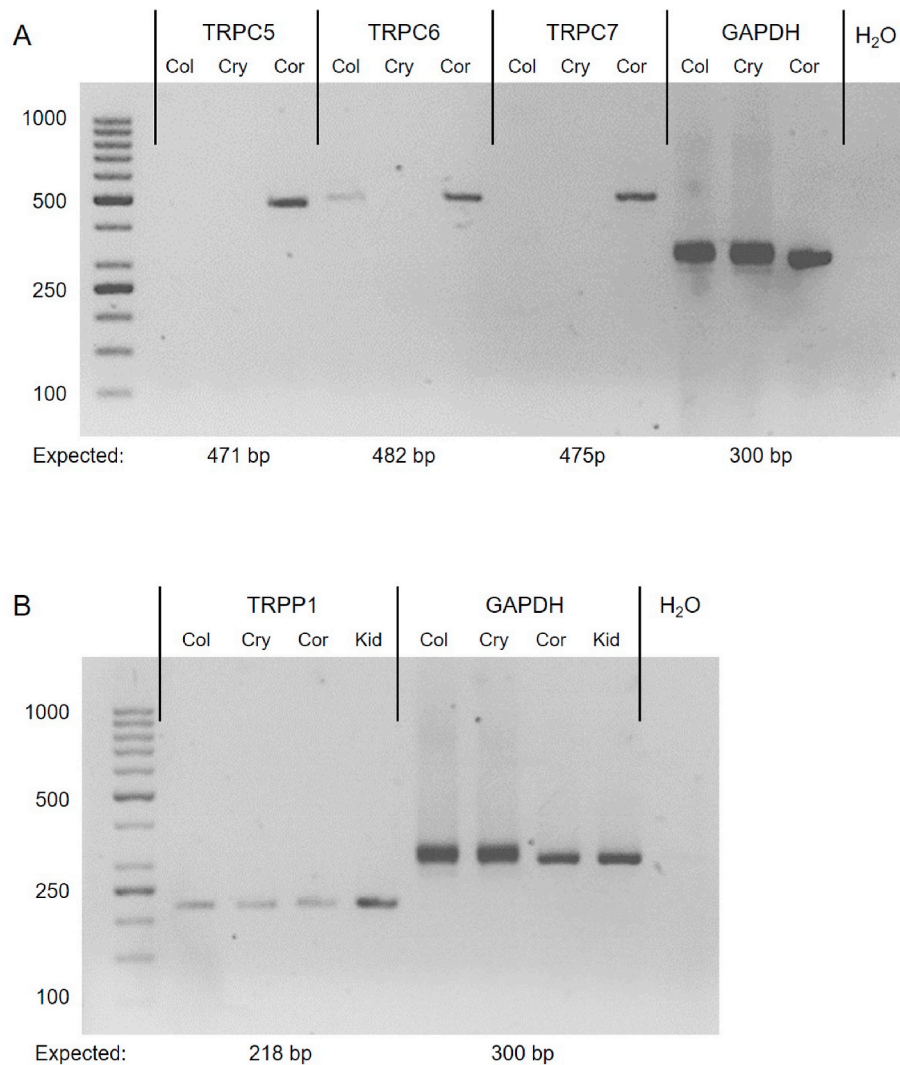


Fig. 8. cDNA prepared from intact colon (Col), isolated colonic crypts (Cry), cerebral cortex (Cor) or kidney (Kid) of Wistar rats by using RT-PCR primers (Table 1) for different TRPC and TRPP channels. The primer free PCR (water) did not reveal any products. Primers for GAPDH were used to proof the quality of the RT-PCR reaction. The DNA ladder (left) used contained cDNA from the range of 50–1000 base pairs (bp). Typical result from three independent experiments (for other gels see Supplementary Figs. 1–6).

differed strongly after basolateral depolarization. Forskolin, the activator of adenylate cyclase(s), induced a pronounced increase in I_{sc} across the apical membrane (Fig. 5A). This is in accordance with the well-known cAMP/protein kinase A-dependent phosphorylation of the CFTR chloride channel followed by Cl^- efflux across the apical membrane (for review see Csanády et al., 2019). In contrast, the response to carbachol, which evokes an increase in I_{sc} in intact tissue driven by a Ca^{2+} -dependent Cl^- secretion (see e.g. Fig. 1), is reverted into a long-lasting negative I_{sc} after basolateral depolarization (Fig. 4). This is preceded by a short rise in the current (Fig. 4B) due to the transient activation of Ca^{2+} -dependent apical Cl^- channels (Schultheiss et al., 2005). At first glance, the strong negative I_{sc} might be well explained by the stimulation of apical Ca^{2+} -dependent K^+ channels, which are involved in the carbachol-induced Cl^- secretion, leading to K^+ efflux. However, the fall in I_{sc} disappeared in Cl^- -free buffer (Fig. 5B). Thus, the known downregulation of Cl^- currents observed after prolonged activation of the Ca^{2+} signaling pathway (Warhurst et al., 1991; Schultheiss et al., 2001) might be involved in this declining I_{sc} .

As the Cl^- secretory response to mucosal ATP could only be revealed when strong Cl^- gradients are present (Fig. 4B), we asked the question if further cation currents across the apical membrane are involved in the ATP-induced increase of I_{sc} . Indeed, the transepithelial I_{sc} induced by

mucosal ATP was suppressed by lanthanides such as La^{3+} (Fig. 3) or Gd^{3+} (Table 2), which inhibit many types of ion channels including nonselective cation channels, e.g. TRP channels (Palasz et al., 2019). In order to identify the ionic species which might flow across the apical membrane, cation substitution experiments were performed with basolaterally depolarized epithelia. These experiments demonstrated that the apical La^{3+} -sensitive cation conductance stimulated by mucosal ATP is both permeable for Na^+ (Fig. 6) as well as for Ca^{2+} (Fig. 7). In principle, this current might be solely carried by a cation flux across apical P2X₇ receptors acting as ligand-gated nonselective cation channels (Burnstock, 2018). We hypothesized that the activation of apical P2X₇ receptors is followed by a secondary activation of other cation channels amplifying the electrical response to the purinergic agonists. Plausible candidates for this ‘amplification’ might be members of the TRP family which are expressed in many cell types (Nilius and Owsianik, 2011). These cation channels possess a voltage-sensor like domain providing them with a (weak) voltage-sensitivity (for review, see Cao, 2020), so they might have been activated by the ATP-induced depolarization of the apical membrane after opening of the P2X₇ channels. Depending on the channel subtype, many other mechanisms are involved in the regulation of TRP channel activity, e.g. interaction with arachidonic acid, Ca^{2+} /calmodulin, G proteins, membrane

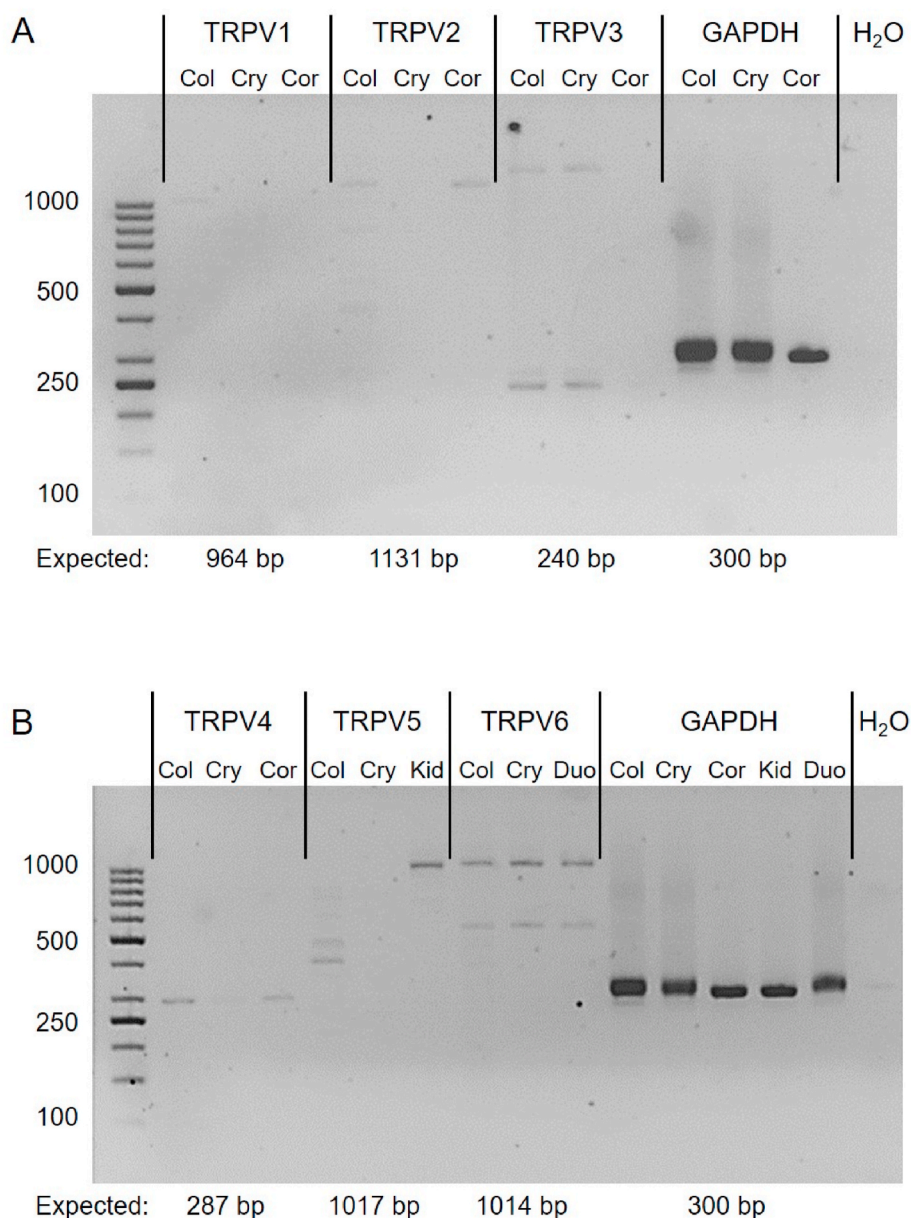


Fig. 9. cDNA prepared from intact colon (Col), isolated colonic crypts (Cry), cerebral cortex (Cor), kidney (Kid), or duodenum (Duo) of Wistar rats by using RT-PCR primers (Table 1) for different TRPV channels. The primer free PCR (water) did not reveal any products. Primers for GAPDH were used to proof the quality of the RT-PCR reaction. The DNA ladder (left) used contained cDNA from the range of 50–1000 base pairs (bp). Typical result from three independent experiments (for other gels see Supplementary Figs. 1–6).

phospholipids, physicochemical stimuli and others (Nilius and Owsianik, 2011).

Thus, we performed a screening for the expression of selected members of the TRP channel family in rat colonic epithelium by RT-PCR experiments. Thereby, we focused on members which might be activated by Ca^{2+} which could flow into the cytosol after P2X_7 activation (Strotmann et al., 2003; Clapham et al., 2005) or by arachidonic acid which might be produced after activation of Ca^{2+} -dependent phospholipase A_2 (Hu et al., 2006). Indeed, the mRNA of several TRP channels such as TRPV3, TRPV4 as well as TRPM4 (and TRPM5) were detected in epithelial homogenates from rat colon (Figs. 8–10).

A further mechanism, by which P2X receptor-mediated cation influx might lead to the opening of many types of TRP channels, is the well-known (modest) voltage dependency of these nonselective cation channels (Cao, 2020). However, a La^{3+} -sensitive I_{sc} could only be evoked by influx of Ca^{2+} from the mucosal compartment mediated by a

Ca^{2+} ionophore, ionomycin, but not by sole depolarization of the apical membrane with K^+ (Fig. 11), indicating a central role of Ca^{2+} in channel activation, whereas a pure depolarization is not sufficient. The observation that the ATP-induced current is inhibited by lanthanides or flufenamate (Fig. 3), two TRP inhibitors (Bencze et al., 2015), together with the broad expression pattern of TRP channels in the colonic epithelium (Figs. 8–10), would fit to the idea that a member (or members) of the TRP ion channel family might be involved in the electrogenic purinergic signaling in colonic epithelium, although the final proof for this hypothesis such as e.g. experiments after selective knock-out of individual TRP channels types is missing.

Beside stimulation by apical purinergic receptors, the (nonselective) cation conductance of the apical membrane is enhanced by forskolin, i.e. after stimulation of intracellular cAMP production. This can be recognized e.g. in Fig. 7, where under control conditions, forskolin induced a strong Ca^{2+} -driven increase in I_{sc} concomitant with a pronounced rise in

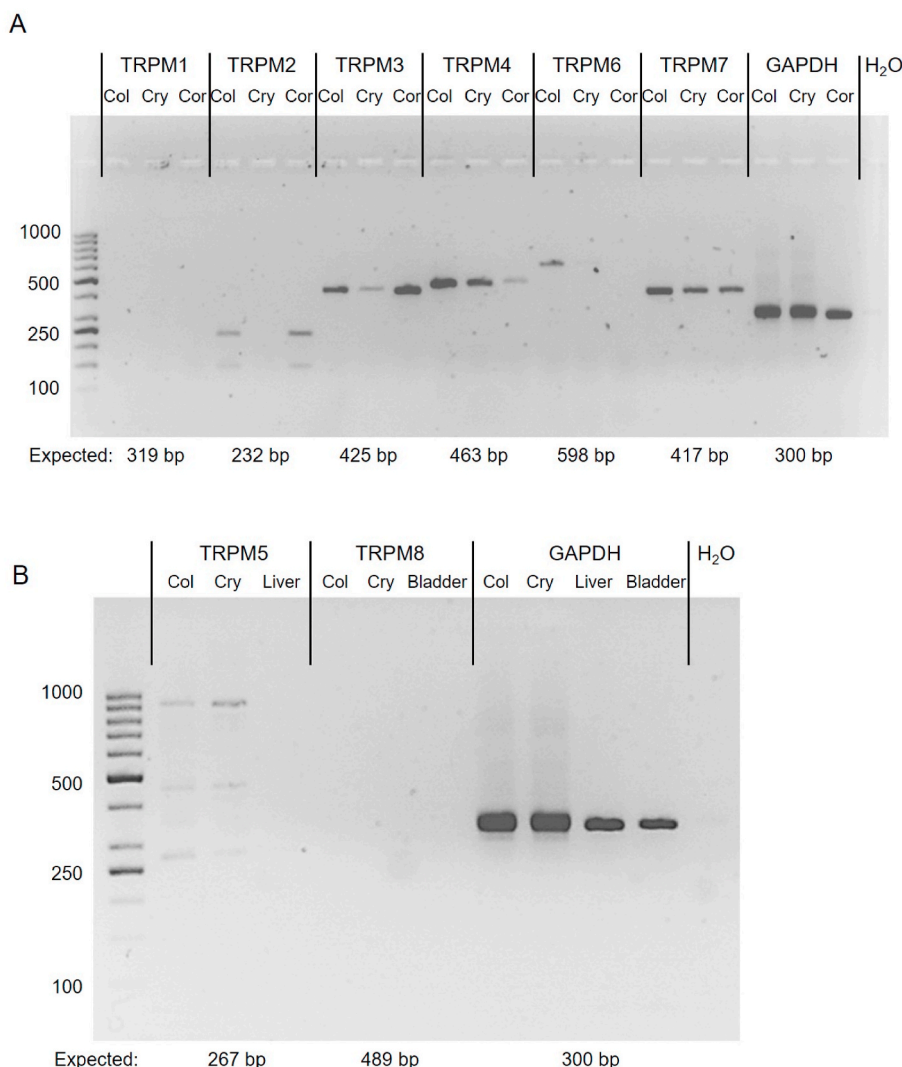


Fig. 10. cDNA prepared from intact colon (Col), isolated colonic crypts (Cry), liver, or urinary bladder of Wistar rats by using RT-PCR primers (Table 1) for different TRPM channels. The primer free PCR (water) did not reveal any products. Primers for GAPDH were used to proof the quality of the RT-PCR reaction. The DNA ladder (left) used contained cDNA from the range of 50–1000 base pairs (bp). Typical result from three independent experiments (for other gels see Supplementary Figs. 1–6).

tissue conductance suggesting cellular damage by Ca^{2+} overload in the cytosol. This current (as well as the tremendous increase in G_i) was (at least numerically) strongly reduced in the presence of La^{3+} (Fig. 7B–Table 4). This effect of forskolin fits well to previous data describing the stimulation of a nonselective cation conductance in rat colonic crypts by cAMP (Siemer and Gögelein, 1993).

Albeit we focused in this study on the ion currents across the apical membrane evoked by ionotropic P2X receptors stimulated with the natural agonist ATP, the G protein-coupled P2Y receptors as possible further targets on epithelial cells (Köttgen et al., 2003) should not be disregarded. Hence, the complex signal cascades after stimulation of intracellular G proteins might also influence ion conductances on the intestinal epithelium after purinergic stimulation.

4.1. Limitations of the present study

A clear limitation of the present study is the missing identification of the TRP channel(s) assumed to be involved in the interaction with apical ionotropic purinergic receptors. At least 10 members of the TRP superfamily have been found in rat colon on the mRNA level. Even, a colocalization in immunohistochemical stainings with P2X₇ receptors would not prove that one of the identified channels is unequivocally

responsible for the assumed interaction. However, we know from our previous immunohistochemical experiments with an antibody against P2X₇ that this receptor is uniformly distributed in the mature cells near the surface of the colonic mucosa, where enterocytes (and a few goblet cells) are the dominating cell type. This allows to grossly localize where the hypothesized “interaction” of ionotropic receptors and TRP channels might take place. A further shortcoming lies in the absence of specific antagonists for most of these channels (see e.g. IUPHAR Guide to pharmacology). Thus, without experiments using selective knock-out of different TRP channels, e.g. by CRISPR-Cas9 gene editing, the question which type of non-selective cation channels is involved remains open.

5. Conclusion

Taken together, mucosal ATP, a well-known ‘danger signal’, activates cation and anion channels via purinergic receptors in the apical membrane. The Ca^{2+} influx via the ionotropic ATP receptor(s) activates Ca^{2+} -dependent K^+ channels (both in the apical and the basolateral membrane) as well as apical Ca^{2+} -dependent Cl^- channels to induce a secretory response as part of the local defence mechanism of the intestinal epithelium. We assume that this effect is ‘amplified’ by an additional Ca^{2+} -dependent activation of La^{3+} -sensitive, nonselective cation

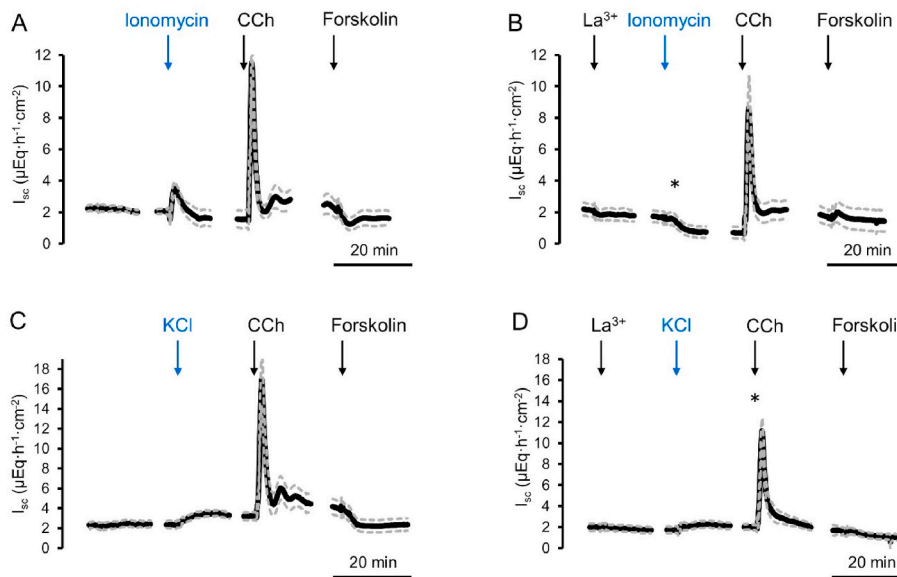


Fig. 11. Effect of ionomycin (1 μM , mucosal; A, B) or KCl (30 mM, mucosal; C, D) on I_{sc} in the absence (A, C) or presence (B, D) of La^{3+} (1 mM, mucosal). As viability control, carbachol (CCh; 50 $\mu\text{mol/l}$, serosal) and forskolin (10 $\mu\text{mol/l}$, mucosal and serosal) were administered. Data shown in panels A and B (as well as C and D) are from experiments performed in adjacent tissue samples from the same animals. Line interruptions are caused by omission of time intervals in order to synchronize the tracings of individual records to the administration of the next drug. Data are means (thick lines) \pm S.E.M. (dashed lines), $n = 6$. * $P < 0.05$ versus response in the absence of La^{3+} . For statistics, see text.

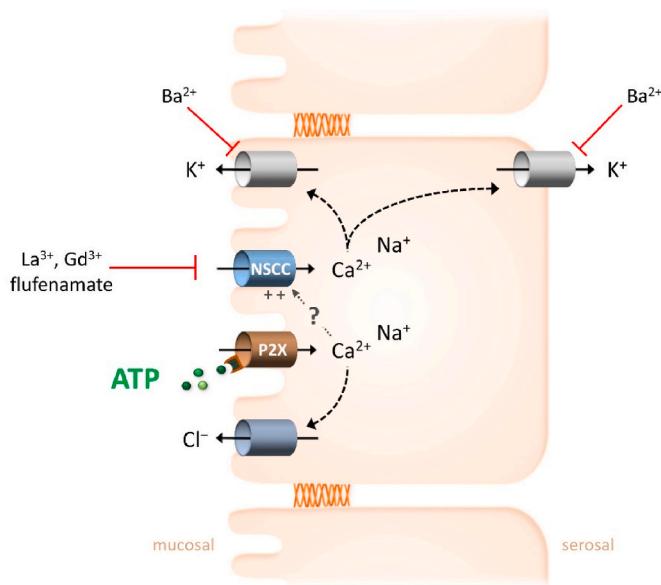


Fig. 12. Working model for the mechanism underlying the transepithelial currents stimulated by mucosal ATP. NSCC: non-selective cation channel.

channels (e.g. members of the TRP family), which further enhance the cation influx across the apical membrane (Fig. 12). ATP is well known to be released from bacteria (including those of the gastrointestinal tract) during their logarithmic growth phase and the detection of extracellular ATP is a powerful tool for control of hygiene (Ihsen et al., 2021). Furthermore, non-selective cation channels such as TRPV3 – beside their role in Ca^{2+} signaling – are known to be involved in the absorption of NH_4^+ resulting from the bacterial fermentation of proteins and other N-containing substrates (Liebe et al., 2021). Thus, the presumed interaction of purine receptors with non-selective cation channels suggested by the present experiments might well serve to identify further functions of these channels such as removal of bacterial metabolites.

CRedit authorship contribution statement

Jasmin Ballout: Writing – review & editing, Writing – original draft, Methodology, Investigation, Formal analysis, Conceptualization. **Martin Diener:** Writing – review & editing, Writing – original draft, Methodology, Investigation, Formal analysis, Conceptualization.

Declaration of competing interest

Purinergic control of apical ion conductance by luminal ATP in rat colonic epithelium. Jasmin Ballout, Martin Diener. The authors declare that there are no competing interests.

Data availability

Data will be made available on request.

Acknowledgements

The diligent technical assistance of Mrs. Brigitta Buß, Bärbel Schmidt and Alice Stockinger is a pleasure to acknowledge. We thank J. Hernandez for linguistic support.

Appendix A. Supplementary data

Supplementary data to this article can be found online at <https://doi.org/10.1016/j.ejphar.2024.176941>.

References

Bader, S., Diener, M., 2018. Segmental differences in the non-neuronal cholinergic system in rat caecum. *Pflügers Arch. Eur. J. Physiol.* 470, 669–679.
 Ballout, J., Claßen, R., Richter, K., Grau, V., Diener, M., 2022. Ionotropic P2X₄ and P2X₇ receptors in the regulation of ion transport across rat colon. *Br. J. Pharmacol.* 179, 4992–5011.
 Bencze, M., Behuliak, M., Vavrinova, A., Zicha, J., 2015. Broad-range TRP channel inhibitors (2-APB, flufenamic acid, SKF-96365) affect differently contraction of resistance and conduit femoral arteries of rat. *Eur. J. Pharmacol.* 765, 533–540.
 Böhme, M., Diener, M., Rummel, W., 1991. Calcium- and cyclic-AMP-mediated secretory responses in isolated colonic crypts. *Pflügers Arch. Eur. J. Physiol.* 419, 144–151.
 Burnstock, G., 2018. Purine and purinergic receptors. *Brain Neurosci. Adv* 2, 1–10.

- Burnstock, G., Wong, H., 1978. Comparison of the effects of UV light and purinergic nerve stimulation on the Guinea-pig taenia coli. *Br. J. Pharmacol.* 62, 293–302.
- Cao, E., 2020. Structural mechanisms of transient receptor potential ion channels. *J. Gen. Physiol.* 152, e201811998.
- Caldwell, R.A., Clemo, H.F., Baumgarten, C.M., 1998. Using gadolinium to identify stretch-activated channels: technical considerations. *Am. J. Physiol.* 275, C619–C621.
- Clapham, D.E., Julius, D., Montell, C., Schultz, G., 2005. International union of pharmacology. XLIX. Nomenclature and structure-function relationships of transient receptor potential channels. *Pharmacol. Rev.* 57, 427–450.
- Cook, D.I., Young, J.A., 1989. Effect of K^+ channels in the apical membrane on epithelial secretion based on secondary active Cl^- transport. *J. Membr. Biol.* 110, 139–146.
- Cook, N.S., Quast, U., 1990. Potassium channel pharmacology. In: Cook, N.S. (Ed.), *Potassium Channels. Structure, Classification, Function and Therapeutic Potential*. Ellis Horwood, New York, pp. 181–255.
- Csanády, L., Vergani, P., Gadsby, D.C., 2019. Structure, gating, and regulation of the CFTR anion channel. *Physiol. Rev.* 99, 707–738.
- Cuthbert, A.W., Hickman, M.E., 1985. Indirect effects of adenosine triphosphate on chloride secretion in mammalian colon. *J. Membr. Biol.* 86, 157–166.
- Dulin, N.O., 2020. Calcium-activated chloride channel ANO1/TMEM16A: regulation of expression and signaling. *Front. Physiol.* 11, 590262.
- Fuchs, W., Larsen, E.H., Lindemann, B., 1977. Current-voltage curve of sodium channels and concentration dependence of sodium permeability in frog skin. *J. Physiol.* 267, 137–166.
- Gögelein, H., Dahlem, D., Englert, H.C., Lang, H.J., 1990. Flufenamic acid, mefenamic acid and niflumic acid inhibit single nonselective cation channels in the rat exocrine pancreas. *FEBS (Fed. Eur. Biochem. Soc.) Lett.* 268, 79–82.
- Gögelein, H., Greger, R., 1986. A voltage-dependent ionic channel in the basolateral membrane of late proximal tubules of the rabbit kidney. *Pflügers Arch. Eur. J. Physiol.* 407 (Suppl. 2), S142–S148.
- Gulbransen, B.D., Bashashati, M., Hirota, S.A., Gui, X., Roberts, J.A., MacDonald, J.A., Muruve, D.A., McKay, D.M., Beck, P.L., Mawe, G.M., Thompson, R.J., Sharkey, K.A., 2012. Activation of neuronal P2X7 receptor-pannexin-1 mediates death of enteric neurons during colitis. *Nat. Med.* 18, 600–604.
- Hu, H.Z., Xiao, R., Wang, C., Gao, N., Colton, C.K., Wood, J.D., Zhu, M.X., 2006. Potentiation of TRPV3 channel function by unsaturated fatty acids. *J. Cell. Physiol.* 208, 201–212.
- Ihsen, J., Jovanovic, N., Sirec, T., Spitz, U., 2021. Real-time monitoring of extracellular ATP in bacterial cultures using thermostable luciferase. *PLoS One* 16, e0244200.
- IUPHAR Guide to pharmacology.** <https://www.guidetopharmacology.org/> (accessed 10 July 2023).
- Keely, S.J., Barrett, K.E., 2022. Intestinal secretory mechanisms and diarrhea. *Am. J. Physiol. Gastrointest. Liver Physiol.* 322, G405–G420.
- Köttgen, M., Löffler, T., Jacobi, C., Nitschke, R., Pavenstädt, H., Schreiber, R., Frische, R., Nielsen, S., Leipziger, J., 2003. P2Y6 receptor mediates colonic NaCl secretion via differential activation of cAMP-mediated transport. *J. Clin. Invest.* 111, 371–379.
- Li, S., Wang, X., Ye, H., Gao, W., Pu, X., Yang, Z., 2010. Distribution profiles of transient receptor potential melastatin- and vanilloid-related channels in rat spermatogenic cells and sperm. *Mol. Biol. Rep.* 37, 1287–1293.
- Liebe, H., Liebe, F., Sponder, G., Hedtrich, S., Stumpff, F., 2021. Beyond Ca^{2+} signalling: the role of TRPV3 in the transport of NH_4^+ . *Pflügers Arch. Eur. J. Physiol.* 473, 1859–1884.
- McGahon, M.K., Fernández, J.A., Dash, D.P., McKee, J., Simpson, D.A., Zholos, A.V., McGeown, J.G., Curtis, T.M., 2016. TRPV2 channels contribute to stretch-activated cation currents and myogenic constriction in retinal arterioles. *Invest. Ophthalmol. Vis. Sci.* 57, 5637–5647.
- Nilius, B., Owsianik, G., 2011. The transient receptor potential family of ion channels. *Genome Biol.* 12, 218.
- Oikawa, M., Saino, T., Kimura, K., Kamada, Y., Tamagawa, Y., Kurosaka, D., Satoh, Y., 2013. Effects of protease-activated receptors (PARs) on intracellular calcium dynamics of acinar cells in rat lacrimal glands. *Histochem. Cell Biol.* 140, 463–476.
- Palasz, A., Segovia, Y., Skowronek, R., Worthington, J.J., 2019. Molecular neurochemistry of the lanthanides. *Synapse* 73, e22119.
- Pouokam, E., Bader, S., Brück, B., Schmidt, B., Diener, M., 2013. ATP-sensitive K^+ channels in rat colonic epithelium. *Pflügers Arch. Eur. J. Physiol.* 465, 865–877.
- Riedel, T., Schmalzing, G., Markwardt, F., 2007. Influence of extracellular monovalent cations on pore and gating properties of P2X₇ receptor-operated single-channel currents. *Biophys. J.* 93, 846–858.
- Schultheiss, G., Diener, M., 1997. Regulation of apical and basolateral K^+ conductances in the rat colon. *Br. J. Pharmacol.* 122, 87–94.
- Schultheiss, G., Ribeiro, R., Diener, M., 2001. Fatty acids inhibit anion secretion in rat colon: apical and basolateral action sites. *Pflügers Arch. Eur. J. Physiol.* 442, 603–613.
- Schultheiss, G., Frings, M., Hollingshaus, G., Diener, M., 2000. Multiple actions of flufenamate on ion transport across the rat distal colon. *Br. J. Pharmacol.* 130, 875–885.
- Schultheiss, G., Siefjediers, A., Diener, M., 2005. Muscarinic receptor stimulation activates a Ca^{2+} -dependent Cl^- conductance in rat distal colon. *J. Membr. Biol.* 204, 117–127.
- Siemer, C., Gögelein, H., 1993. Effects of forskolin on crypt cells of rat distal colon. Activation of nonselective cation channels in the crypt base and of a chloride conductance pathway in other parts of the crypt. *Pflügers Arch. Eur. J. Physiol.* 424, 321–328.
- Stokes, L., Surprenant, A., 2009. Dynamic regulation of the P2X₄ receptor in alveolar macrophages by phagocytosis and classical activation. *Eur. J. Immunol.* 39, 986–995.
- Strotmann, R., Schultz, G., Plant, T.D., 2003. Ca^{2+} -dependent potentiation of the nonselective cation channel TRPV4 is mediated by a C-terminal calmodulin binding site. *J. Biol. Chem.* 278, 26541–26549.
- Virginio, C., Church, D., North, R.A., Surprenant, A., 1997. Effects of divalent cations, protons and calmidazolium at the rat P2X₇ receptor. *Neuropharmacology* 36, 1285–1294.
- Warhurst, G., Higgs, N.B., Tonge, A., Turnberg, L.A., 1991. Stimulatory and inhibitory actions of carbachol on chloride secretory responses in human colonic cell line T84. *Am. J. Physiol.* 261, G220–G228.
- Wynn, G., Ma, B., Ruan, H.Z., Burnstock, G., 2004. Purinergic component of mechanosensory transduction is increased in a rat model of colitis. *Am. J. Physiol. Gastrointest. Liver Physiol.* 287, G647–G657.
- Yang, X.R., Lin, M.J., McIntosh, L.S., Sham, J.S.K., 2016. Functional expression of transient receptor potential melastatin- and vanilloid related channels in pulmonary arterial and aortic smooth muscle. *Am. J. Physiol. Lung Cell Mol. Physiol.* 290, L1267–L1276.